

# High-accuracy measurement of cladding noncircularity based on phase velocity difference between acoustic polarization modes

Sun Do Lim<sup>1,2,\*</sup>, Hyun Chul Park<sup>1</sup>, Kwanil Lee<sup>2</sup>, Sang Bae Lee<sup>2</sup>, and Byoung Yoon Kim<sup>1</sup>

<sup>1</sup>Department of Physics, Korea Advanced Institute of Science and Technology (KAIST), Daejeon, 305-701, South Korea

<sup>2</sup>Photonics Research Laboratory, Korea Institute of Science and Technology (KIST), Seoul, 136-791, South Korea

\* [sdlim1976@gmail.com](mailto:sdlim1976@gmail.com)

**Abstract:** A high-accuracy measurement method for the noncircularity (ellipticity) of silica glass fibers is demonstrated. This method makes use of the phase velocity difference between two eigen polarization modes of the lowest-order acoustic flexural wave in an optical fiber. The relationship between the acoustic phase velocity difference and the fiber ellipticity is formulated. Three types of optical fibers were examined; photonic crystal fiber, elliptical core fiber, and standard single-mode fiber. Fiber ellipticity of less than 0.001 was successfully measured.

©2010 Optical Society of America

**OCIS codes:** (060.2310) Fiber optics; (230.1040) Acousto-optical devices; (060.2300) Fiber measurements; (120.3180) Interferometry.

---

## References and links

1. B. Langli, and K. Bløtekjær, "Effect of acoustic birefringence on acoustooptic interaction in birefringent two-mode optical fibers," *J. Lightwave Technol.* **21**(2), 528–535 (2003).
2. S. D. Lim, H. C. Park, I. K. Hwang, and B. Y. Kim, "Combined effects of optical and acoustic birefringence on acousto-optic mode coupling in photonic crystal fiber," *Opt. Express* **16**(9), 6125–6133 (2008).
3. M. W. Haakestad, and H. E. Engan, "Acoustooptic characterization of a birefringent two-mode photonic crystal fiber," *Opt. Express* **14**(16), 7319–7328 (2006).
4. D.-I. Yeom, P. Steinvurzel, B. J. Eggleton, S. D. Lim, and B. Y. Kim, "Tunable acoustic gratings in solid-core photonic bandgap fiber," *Opt. Express* **15**(6), 3513–3518 (2007).
5. H. M. Presby, "Ellipticity measurement of optical fibers," *Appl. Opt.* **15**(2), 492–494 (1976).
6. H. Wang, "Theory and experiments on diffraction patterns of an optical fiber with slight ellipticity: a perturbation method," *J. Opt. Soc. Am. A* **13**(6), 1199–1203 (1996).
7. R. James, Rochester, "Measurement of optical fiber diameter," United States Patent US5264909 <http://www.freepatentsonline.com/5264909.pdf>
8. N. Gisin, R. Passy, and B. Perny, "Optical Fiber Characterization by Simultaneous Measurement of the Transmitted and Refracted Near Field," *J. Lightwave Technol.* **11**(11), 1875–1883 (1993).
9. J. Jasapara, E. Monberg, F. DiMarcello, and J. W. Nicholson, "Accurate noncontact optical fiber diameter measurement with spectral interferometry," *Opt. Lett.* **28**(8), 601–603 (2003).
10. J. C. Jasapara, S. Wielandy, and A. D. Yablon, "Fourier domain optical coherent tomography – a new platform for measurement of standard and microstructured fiber dimension," *IEE Proc., Optoelectron.* **153**(5), 229–234 (2006).
11. H. E. Engan, B. Y. Kim, J. N. Blake, and H. J. Shaw, "Propagation and optical interaction of guided acoustic waves in two-mode optical fibers," *J. Lightwave Technol.* **6**(3), 428–436 (1988).
12. S. D. Lim, H. C. Park, and B. Y. Kim, "Twist effect on spectral properties of two-mode fiber acousto-optic filters," *Opt. Express* **16**(17), 13042–13051 (2008).
13. M. W. Haakestad, and H. E. Engan, "Acoustooptic properties of a weakly multimode solid core photonic crystal fiber," *J. Lightwave Technol.* **24**(2), 838–845 (2006).

---

## 1. Introduction

The uniform ovality of an optical fiber cladding is known as cladding noncircularity (ellipticity, which is defined in Eq. (2)). With the use of optical fibers in specialty applications, even a small ellipticity can have a significant influence on the performance of the applications, particularly those utilizing cladding-guided modes. The deformation in the cladding geometry can break the mode symmetry of cladding-guided modes, thereby broadening the spectral linewidth in narrow-band filter applications and/or deteriorating the

sensitivity in sensor applications. Cladding noncircularity is also detrimental to all-fiber devices and sensors when they are based on an acoustic grating. Since the cladding ellipticity is a major source of the acoustic linear birefringence, it can lead to unpredictable output spectrum such as resonance peak splitting depending on the acoustic bias condition [1–4]. In order to reduce and control the negative effects of cladding noncircularity on the performance of the applications, cladding noncircularity has to be investigated in detail.

In this paper, we propose and demonstrate a new method for the high-accuracy measurement of optical fiber ellipticity. This method utilizes the lowest-order flexural acoustic waves in an optical fiber. Since the acoustic waves excited along the axes of the fiber ellipse have different phase velocity, the phase difference between them provides information of the ellipticity. A formula converting the measured phase difference to the fiber ellipticity was devised based on the acoustic dispersion relation. The ellipticity measurements were performed for three different types of optical fibers: photonic crystal fiber (PCF), elliptical-core fiber and standard single-mode fiber (SMF). The measurement results were compared with those by an optical fiber geometry analyzer, and they show good agreement. This method exhibits a nanometer level accuracy and precision of up to  $\pm 3$  nm for the ellipticity measurement of the standard SMF, and it turned out that the ellipticity of the SMF is less than 0.001.

It is worth noting that to date, many optical methods such as scattering and diffraction patterns, shadowing techniques, refracted near field, and spectral interferometry have been used to measure the fiber dimension [5–10]. They can also be exploited to provide the fiber ellipticity, but this method shows an enhanced accuracy and precision for the ellipticity measurement compared to the above-listed techniques. However, this cannot be used for real-time monitoring of the fiber ellipticity during the fiber drawing process because it is a contact method.

## 2. Theory

### *Acoustic dispersion relation*

Optical fibers are excellent acoustic media as well as superior waveguides for light transmission since optical fibers consist of fused silica that is a solid, isotropic, homogeneous, and lossless material. There exist three kinds of acoustic waves in optical fibers: longitudinal, torsional, and flexural modes. In the experiment, we used the flexural mode, particularly the lowest-order flexural mode. The acoustic flexural mode is doubly degenerated (x- and y-polarized) for the optical fiber with a perfect circularity in cladding geometry. An acoustic wave equation provides a dispersion relation for the lowest-order flexural mode [11]. The dispersion relation in a low-frequency region where acoustic wavelength is larger than the fiber diameter ( $\lambda \gg D$ ) can be expressed by

$$\frac{fD}{3764(m/s)} \approx 2.546 \left( \frac{D}{\lambda} \right)^2 - 2.372 \left( \frac{D}{\lambda} \right)^3 \quad (1)$$

where,  $f$  is the acoustic frequency,  $D$  is the fiber diameter, and  $\lambda$  is the acoustic wavelength. (Plotted in Fig. 1).

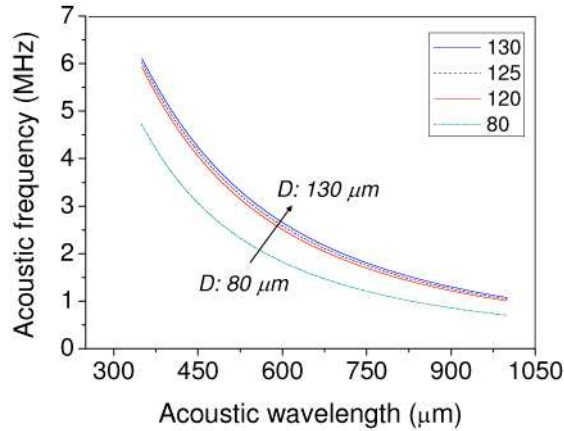


Fig. 1. Acoustic dispersion relation

This implies that the velocity of the acoustic flexural mode relies on the fiber diameter. In a real situation, the optical fiber cladding cannot be perfectly circular. The ellipticity in the cladding geometry is a major source of the acoustic linear birefringence, which breaks the degeneracy between the acoustic polarization modes. The axes of the birefringence are coincided with the major and minor axes of the cladding ellipse. Thus, the two eigen acoustic polarization modes have different acoustic dispersion relations owing to the effectively different fiber diameter. The effective fiber diameters are depicted in Fig. 2.

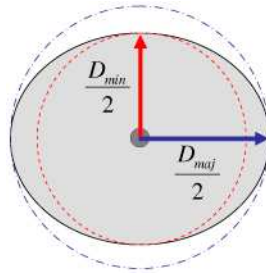


Fig. 2. Description of the effective diameters of the optical fiber with ellipticity

In this paper, the ellipticity,  $\varepsilon$  is defined as follows.

$$\varepsilon = \frac{D_{major} - D_{minor}}{(D_{major} + D_{minor})/2} = \frac{\Delta D}{D} \quad (2)$$

#### Acoustic phase difference

A simple fiber interferometer was used for the measurement of the acoustic phase difference between the acoustic polarization modes, and is depicted in Fig. 3 (b). A flexural acoustic wave in the low frequency region approximately introduces a traveling sinusoidal displacement along the fiber. Thus, when the flexural acoustic wave propagates along the test fiber, two reflected light fields  $E_1$  (from the cleaved end-face of the sensing fiber) and  $E_2$  (from the surface of the test fiber) interfere and produce sinusoidal intensity modulation as a function of time. The governing equation is written as

$$I = |E_1 + E_2 e^{2ikd}|^2 \quad \text{where, } d = d_0 + a_0 \sin(k_a l - \omega_a t) \quad (3)$$

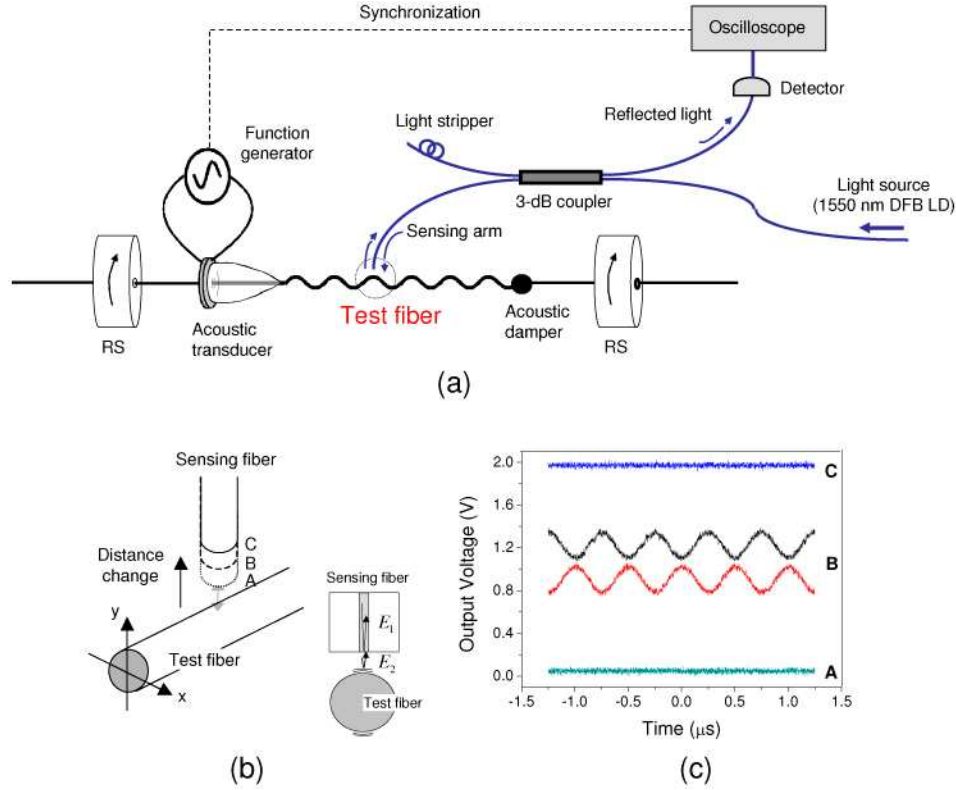


Fig. 3. (a) Experimental setup for the measurement of fiber ellipticity (RS: rotation stage) (b) Measurement of interference with changing the distance between the sensing fiber and the test fiber (c) Output signal patterns for different distances between the sensing fiber and the test fiber. ( $E_1$  and  $E_2$  denote reflected electric fields)

In Eq. (3),  $k$  is the propagation constant of the light.  $d_0$  is the distance between the sensing fiber of the coupler and the test fiber.  $a_0$ ,  $k_a$ ,  $l$ , and  $\omega_a$  are the oscillation amplitude, the propagation constant, the propagation length, and the angular frequency of the acoustic wave, respectively. It can be rewritten as

$$I = E_1^2 + E_2^2 + 2E_1E_2 \cos(2kd_0 + 2ka_0 \sin(k_a l - \omega_a t)) \quad (4)$$

If  $2kd_0$  can be adjusted to be  $(n + 1/2)\pi$ , ( $n = 1, 2, 3, \dots$ ), then Eq. (4) is approximated as following since  $2ka_0$  is relatively small

$$I \cong E_1^2 + E_2^2 \pm 4E_1E_2ka_0 \sin(k_a l - \omega_a t) \quad (5)$$

This is representative of case 'B' shown in Fig. 3(c). In the case that  $2kd_0$  is  $n\pi$ , and  $2ka_0$  is also relatively small, then Eq. (4) will be simplified as follows

$$I \cong E_1^2 + E_2^2 \pm 2E_1E_2 \quad (6)$$

As are cases 'A' and 'C' as shown in Fig. 3(c). As one can see in Eq. (4), the phase of the acoustic wave as a function of distance and time can be written by  $\varphi = k_a l - \omega_a t$ . For two acoustic polarization modes, the phase difference  $\Delta\varphi$  for a given time can be written as

$$\Delta\varphi = |\Delta k_a \cdot l| \quad \text{where, } \Delta k_a = 2\pi \cdot \left( \frac{\Lambda_{maj} - \Lambda_{min}}{\Lambda_{maj} \cdot \Lambda_{min}} \right) \cong 2\pi \cdot \frac{\Delta\Lambda}{\Lambda^2} \quad (7)$$

Here,  $\Lambda_{maj}$  and  $\Lambda_{min}$  are the effective acoustic wavelengths for the two acoustic polarization modes.

*Formula on ellipticity with a newly defined parameter  $\alpha$*

Equation (8) was derived by substituting  $D$  with  $D + \Delta D$  and  $\Lambda$  with  $\Lambda + \Delta \Lambda$  in Eq. (1) and using the Taylor expansion. The ellipticity,  $\varepsilon$  can be written as

$$\varepsilon = \frac{\Delta D}{D} \approx \Lambda \cdot \frac{5.092 \cdot \Lambda - 7.116 \cdot D}{2.546 \cdot \Lambda - 4.744 \cdot D} \cdot \left( \frac{\Delta \varphi}{2\pi \cdot l} \right) = \alpha \cdot \left( \frac{\Delta \varphi}{2\pi \cdot l} \right) \quad (8)$$

The detailed derivation processes are given in the Appendix. The newly defined proportionality constant  $\alpha$  here relies on the applied acoustic frequency and the mean fiber diameter, which are tabulated in Table 1.

**Table 1. The proportionality constant,  $\alpha$  ( $\times 10^{-3} m$ )**

		Applied acoustic frequency				
		1 MHz	2 MHz	3 MHz	4 MHz	5 MHz
Mean fiber diameter	120 $\mu m$	2.1460	1.5324	1.2714	1.1280	1.0506
	125 $\mu m$	2.1909	1.5657	1.3009	1.1570	1.0775
	130 $\mu m$	2.2349	1.5985	1.3302	1.1863	1.1103

It is worth noting that there is an error in the value of  $\alpha$  due to some approximations as appeared in Fig. 4.

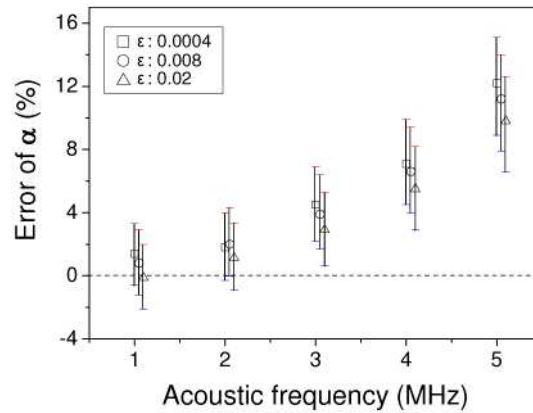


Fig. 4. Errors in the value of  $\alpha$  as a function of the applied acoustic frequency for optical fibers with different ellipticities

The vertical axis denoted by ‘Error of  $\alpha$ ’ in Fig. 4 represents a deviation of the value  $\alpha$  from the one directly obtained by Eq. (1), and it tends to rise as the applied acoustic frequency increases. The error margin also reflects possible additional error that may be introduced by the difference of the actual diameter of the test fibers from the nominal diameter of 125  $\mu m$ . Here, the difference in diameter is assumed to be  $\pm 4\%$ . As one can see in Fig. 4, it is preferable to use the lower acoustic frequency for high precision. However, since it is advantageous to apply the higher acoustic frequency to the fiber to get larger acoustic phase difference, there is a trade-off between them.

### 3. Experiment and analysis

Figure 3(a) illustrates the experimental setup. The acoustic transducer consists of a PZT thin disk, and a glass horn. The glass horn has a hollow with 140- $\mu m$  diameter along its conical center allowing the test optical fiber to be inserted into the hollow and removed without destructing it. The PZT generates an acoustic shear wave by converting AC voltage applied from an electric function generator. The glass horn takes the role of a lens focusing the

acoustic energy on the fiber, thereby introducing the flexural acoustic wave along the fiber. The acoustic damper prevents back reflection of the acoustic wave by absorbing the acoustic energy. The acoustic vibration direction along the fiber can be controlled by two rotation stages holding the fiber. Note that it is important that the fiber should be untwisted when the fiber is mounted. The measurement system consists of a 1550-*nm* laser source (distributed feedback laser diode, DFB LD), a 3-dB coupler, and a photo-detector. The light from the DFB LD goes into the sensing arm through the 3-dB coupler with 3-dB loss. Part of the light reflects on the fiber end of the arm and the rest of the light goes into the air. Then, a part of the light propagating in the air also reflects on the oscillating surface of the test fiber and goes back to the sensing fiber of the 3-dB coupler. Two reflected lights that are measured with the photo detector interfere with each other and produce sinusoidal intensity modulation as a function of time, which reflects the acoustic oscillation. Note that the temporal phase difference of the modulated output signals is equivalent to the spatial phase difference of the acoustic waves at a distance of propagation. The instability of electronic instruments such as an oscilloscope and a photo-detector was not considered because the time jitter of the devices is much smaller compared to the time scale measurement. We measured the output signals for every 5° of axial rotation and found the maximum phase difference by comparing them. It is obvious that the maximum phase difference takes place between two signals respectively measured at each axis of the fiber ellipse. The variation of the phase difference is fast around the 45°-diagonal directions with respect to the ellipse axes. On the other hand, the gradient of the phase variation is almost zero around each axis, which implies that the 5° interval is acceptable for the determination of the maximum phase difference.

In this experiment, three different types of optical fibers were used. One is a photonic crystal fiber (ESM-12-01 PCF, Crystal fiber A/S), the second is an elliptical-core two mode fiber (e-core TMF), and the third is a standard SMF (Corning SMF 28). It was previously found that the optical fibers are noncircular in the cladding geometry but axially uniform in length within a few tens of centimeter length [2,12]. The cladding diameter of 125  $\mu\text{m}$  was used for the test optical fibers. Figure 5 shows two intensity modulated signals exhibiting the maximum temporal phase difference for the PCF. The sensing fiber was located at the distance of 2.71 *cm* from the tip of the glass horn, and a 3.3-*MHz* acoustic wave was applied to the fiber.

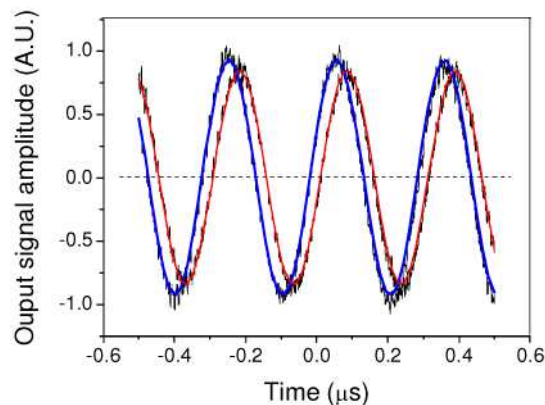


Fig. 5. Intensity modulation signals exhibiting maximal temporal phase difference for the PCF at an applied acoustic frequency of 3.3 *MHz*, Fitting curves are overlaid

According to Eqs. (1) and (8), the value of  $\alpha$  is about  $1.249 \times 10^{-3}$  in this case. The temporal phase difference in the figure was measured to be about 0.0286  $\mu\text{s}$  for the 0.303- $\mu\text{s}$  time period. Taking the parameters into account, the PCF ellipticity was determined to be  $0.00435 \pm 0.00022$ . It means that the diameter difference between the major and the minor axes is about 0.54  $\mu\text{m}$  for the 125- $\mu\text{m}$  mean fiber diameter. It should be noted that the air holes in the PCF has little influence on the acoustic dispersion relation. The presence of the

air holes reduces not only the mass but also the restoring force. The former one makes the acoustic phase velocity faster and the latter one does it slower. As a consequence, net effect by air-hole structure becomes very small and the dispersion relation of the PCF is almost the same as that of the conventional fiber [13]. The ellipticity measurement for the same PCF was carried out under a different acoustic frequency of 4.3 MHz and propagation length of 2.5 cm. In this case, the value of  $\alpha$  is about  $1.1276 \times 10^{-3}$ . The temporal phase difference was measured to be about 0.0232  $\mu\text{s}$  on the 0.2326- $\mu\text{s}$  time period. In this case, the ellipticity of the PCF was determined to be  $0.0045 \pm 0.00036$ , and it shows good agreement with the former results. The same result was also obtained by the scanning electron microscope (SEM) images of the PCF cross sections, which is about 0.0043. Next, the ellipticity measurement for the e-core TMF was performed. In this case, the acoustic frequency and propagation length were 1 MHz and 5.05 cm, respectively, and about 0.111- $\mu\text{s}$  temporal phase difference was obtained. Based on these parameters, the fiber ellipticity was obtained to be  $0.00482 \pm 0.0001$ . Substantially the same result was also obtained by using a fiber geometry analyzer, which is  $0.005 \pm 0.0005$ . Lastly, the corning SMF 28 fiber whose ellipticity was estimated to be less than 0.001 by the fiber geometry analyzer was measured. Figure 6 shows the two selected signals exhibiting the maximum phase difference after 17.1-cm propagation for 2-MHz acoustic frequency. The temporal phase difference in the figure was about 0.047  $\mu\text{s}$  on the 0.5- $\mu\text{s}$  time period.

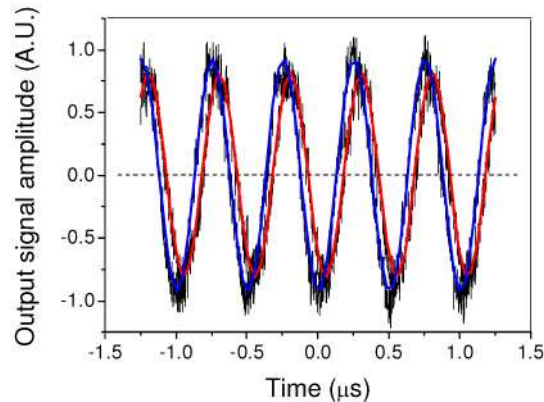


Fig. 6. Intensity modulation signals with maximal temporal phase difference at 2 MHz for standard SMF, Fitting curves are overlaid.

In this case, the value of  $\alpha$  is about  $1.5657 \times 10^{-3}$ . Taking these parameters into account, the ellipticity of the fiber is determined to be  $0.00086 \pm 0.00002$ . This means that the diameter difference between the major and the minor axes is about  $0.107 \pm 0.003 \mu\text{m}$ . All measurement results are tabulated and compared (Table 2).

Table 2. Comparison of our measurements with the results of fiber geometry analyzer

	Measurements	Fiber geometry analyzer
PCF	$0.00435 \pm 0.00022$	0.0043 (from SEM images)
E-core TMF	$0.00482 \pm 0.0001$	$0.005 \pm 0.0005$
Standard SMF	$0.00086 \pm 0.00002$	Less than 0.001

#### 4. Conclusion

A new measurement method for the fiber ellipticity was proposed and demonstrated. A simple formula on the fiber ellipticity was derived from the acoustic dispersion relation. Three types of optical fibers were measured, and the results are in good agreement with those obtained by an optical fiber geometry analyzer and scanning electron microscope images. A fiber ellipticity of less than 0.001 was successfully measured.

## Appendix

### Derivation of the formula on ellipticity

Substituting  $D$  with  $D+\Delta D$  and  $\Lambda$  with  $\Lambda+\Delta\Lambda$ , Eq. (1) becomes

$$\frac{f(D+\Delta D)}{3764(m/s)} = 2.546\left(\frac{D+\Delta D}{\Lambda+\Delta\Lambda}\right)^2 - 2.372\left(\frac{D+\Delta D}{\Lambda+\Delta\Lambda}\right)^3$$

and it can be rewritten as

$$\frac{f \cdot (D+\Delta D)}{3764(m/s)} = 2.546\left(\frac{D}{\Lambda}\right)^2 \left(1+\frac{\Delta D}{D}\right)^2 \left(1+\frac{\Delta\Lambda}{\Lambda}\right)^{-2} - 2.372\left(\frac{D}{\Lambda}\right)^3 \left(1+\frac{\Delta D}{D}\right)^3 \left(1+\frac{\Delta\Lambda}{\Lambda}\right)^{-3}$$

Since  $\Delta D/D$  and  $\Delta\Lambda/\Lambda$  are much smaller than unity, this equation can be simplified after the Taylor expansion with approximations as

$$\frac{f \cdot \Delta D}{3764(m/s)} \approx \left[ 2 \times 2.546 \left(\frac{D}{\Lambda}\right)^2 - 3 \times 2.372 \left(\frac{D}{\Lambda}\right)^3 \right] \cdot \left( \frac{\Delta D}{D} - \frac{\Delta\Lambda}{\Lambda} \right)$$

Using Eq. (1), it can be written by

$$\frac{\Delta D}{D} \approx \frac{5.092\Lambda - 7.116D}{2.546\Lambda - 4.744D} \left( \frac{\Delta\Lambda}{\Lambda} \right)$$

By the acoustic wavelength and the phase difference relation in the Eq. (7), the ellipticity can be rewritten as

$$\varepsilon = \frac{\Delta D}{D} \approx \Lambda \cdot \frac{5.092\Lambda - 7.116D}{2.546\Lambda - 4.744D} \cdot \left( \frac{\Delta\varphi}{2\pi \cdot l} \right)$$